Annals of Medicine

ISSN: (Print) (Online) Journal homepage: www.tandfonline.com/journals/iann20

Propyl gallate induces human pulmonary fibroblast cell death through the regulation of Bax and caspase-3

Woo Hyun Park

To cite this article: Woo Hyun Park (2024) Propyl gallate induces human pulmonary fibroblast cell death through the regulation of Bax and caspase-3, Annals of Medicine, 56:1, 2319853, DOI: 10.1080/07853890.2024.2319853

To link to this article: https://doi.org/10.1080/07853890.2024.2319853

Published online: 19 Feb 2024.

ANNALS OF MEDICINE
2024, VOL. 56, NO. 1, 2319853
https://doi.org/10.1080/07853890.2024.2319853

RESEARCH ARTICLE

OPEN ACCESS Check for updates

Propyl gallate induces human pulmonary fibroblast cell death through the regulation of Bax and caspase-3

Woo Hyun Park

Department of Physiology, Medical School, Jeonbuk National University, Jeonju, Jeollabuk, Republic of Korea

ABSTRACT

Propyl gallate (PG) has been found to exert an inhibitory effect on the growth of different cell types, including lung cancer cells. However, little is known about the cytotoxicological effects of PG specifically on normal primary lung cells. The current study examined the cellular effects and cell death resulting from PG treatment in human pulmonary fibroblast (HPF) cells. DNA flow cytometry results demonstrated that PG (100–1,600 μM) had a significant impact on the cell cycle, leading to G1 phase arrest. Notably, 1,600 μM PG slightly increased the number of sub-G1 cells. Additionally, PG (400–1,600 μM) resulted in the initiation of cell death, a process that coincided with a loss of mitochondrial membrane potential (MMP; ΔΨm). This loss of MMP (ΔΨm) was evaluated using a FACS cytometer. In PG-treated HPF cells, inhibitors targeting pan-caspase, caspase-3, caspase-8, and caspase-9 showed no significant impact on the quantity of annexin V-positive and MMP (ΔΨm) loss cells. The administration of siRNA targeting Bax or caspase-3 demonstrated a significant attenuation of PG-induced cell death in HPF cells. However, the use of siRNAs targeting p53, Bcl-2, or caspase-8 did not exhibit any notable effect on cell death. Furthermore, none of the tested MAPK inhibitors, including MEK, c-Jun N-terminal kinase (JNK), and p38, showed any impact on PG-induced cell death or the loss of MMP (ΔΨm) in HPF cells. In conclusion, PG induces G1 phase arrest of the cell cycle and cell death in HPF cells through apoptosis and/or necrosis. The observed HPF cell death is mediated by the modulation of Bax and caspase-3. These findings offer insights into the cytotoxic and molecular effects of PG on normal HPF cells.

Abbreviations: HPF: human pulmonary fibroblast; PG: propyl gallate; MMP (ΔΨm): mitochondrial membrane potential; Z-VAD-FMK: benzyloxycarbonyl-Val-Ala-Asp-fluoromethylketone; Z-DEVD-FMK: benzyloxycarbonyl-Asp-Glu-Val-Asp-fluoromethylketone; Z-IETD-FMK: benzyloxycarbonyl-Ile-Glu-Thr-Asp-fluoromethylketone; Z-LEHD-FMK: benzyloxycarbonyl-Leu-Glu-His-Asp-fluoromethylketone; MAPK: mitogen-activated protein kinase; MEK: MAP kinase or ERK kinase; ERK: extracellular signal-regulated kinase; JNK: c-Jun N-terminal kinase; FBS: fetal bovine serum; PI: propidium iodide; FITC: fluorescein isothiocyanate; siRNA: small interfering RNA

ARTICLE HISTORY
Received 11 July 2023
Revised 14 January 2024
Accepted 11 February 2024

KEYWORDS
Human pulmonary fibroblast; propyl gallate; cell death; cell cycle; caspase; mitogen-activated protein kinase

1. Introduction

Propyl gallate (PG; 3,4,5-trihydroxybenzoic acid propyl ester) has been used for decades as a certified additive in food, cosmetics, and pharmaceutical preparations [1]. PG not only has subdued toxicity but also has various advantageous properties for the function of both tissues and cells. A number of studies have identified the benefits of PG as an antioxidant [2, 3] and a chemopreventive agent [4]. However, other studies have reported that treatment with 500 μM PG shows pro-oxidant properties *via* increasing the amount of 8-oxo-7,8-dihydro-2′-deoxyguanosine (8-oxodG) in HL-60 leukemia cells [5] and PG (500–2,000 μM) has been shown to be toxic to freshly isolated rat hepatocytes by damaging the mitochondria [6]. PG also prevents respiration and nucleic acid synthesis in microorganisms [7]. Interestingly, the antioxidative and cytoprotective properties of PG may switch to pro-oxidative and cytotoxic properties in the presence of Cu(II) [8]. PG has been shown to augment human diploid fibroblast growth at a concentration of 10^{-8} M but to diminish their growth at a concentration of 10^{-6}

CONTACT Woo Hyun Park parkwh71@jbnu.ac.kr Department of Physiology, Medical School, Jeonbuk National University, Jeonju, Jeollabuk, 54907, Republic of Korea

M or greater [9]. As there is discrepancy between these extraneous effects of PG, further studies are needed to re-evaluate its function and properties in cells and tissues.

Eukaryotic cell cycle is the series of events that consists of four distinct phases: G1 phase, S phase, G2 phase and M phase [10, 11]. Management of the cell cycle is important to the cell proliferation and survival and is involved in the procedures of the detection and repair of genetic impairment as well as the avoidance of uncontrolled cell division [10, 11]. Apoptosis is a cellular response to cytotoxic agents and is typically comprised of two central signaling pathways: the mitochondrial and cell death receptor pathways [12]. The commencement of apoptosis in the mitochondrial pathway is prompted or accompanied by increased levels of proapoptotic proteins, including Bax, and decreased levels of antiapoptotic proteins, such as Bcl-2, subsequently leading to the mitochondrial membrane potential (MMP; ΔΨm) loss [13]. As the p53 protein regulates the expression of Bax and Bcl-2, the status of p53 is tightly related to apoptosis [14]. The mitochondrial pathway is marked by the efflux of cytochrome *c*, which moves from the mitochondria to the cytosol, where it forms an apoptosome complex, along with apoptotic protease-activating factor 1 and caspase-9. This subsequently leads to the stimulation of caspase-3 [12, 15]. The other cell death pathway, which is associated with cell death receptors, is distinguished by the interaction of cell death ligands with their death receptors, initiating the activities of caspase-8 and caspase-3 [16]. The activated caspase-3 systematically breaks down cells by dismantling fundamental proteins, including poly (ADP-ribose) polymerase.

Mitogen-activated protein kinases (MAPKs) are evolutionarily conserved signaling proteins that facilitate responses to various stimuli. Extracellular signal-regulated kinases (ERK1/ERK2), the c-Jun N-terminal kinase/stress-activated protein kinases (JNK/SAPK), and the p38 kinases are the three principal MAPK components present in eukaryotes [17]. Each distinct MAPK pathway has specific upstream activators and substrates [18]. Several MAPK pathways are involved in cell growth, cell survival, differentiation, and cell death [19]. Typically, the activation of ERK is related to cell survival, rather than cell death [20]. In addition, oxidative stress can induce the ERK signaling pathway through specific phosphorylation of the ERK enzyme [21]. The activities of both JNK and p38 are ordinarily stimulated by mild oxidative stress, and their activation can induce cell death [22, 23]. Furthermore, the activities of MAPKs are regulated by subsidiary MAPK phosphatases, which are explicitly controlled by reactive oxygen species [24].

Lung cancer is the leading cause of cancer-related death worldwide [25]. Due to the limited number of existing drugs available, many new treatment strategies are still being evaluated [26]. Studies of the molecular mechanisms of cytotoxic drug action have shed light on the management of lung cancer. PG has anti-growth effects in numerous cell types, including cells in the testis [27], endothelial cells [28, 29], leukemia cells [30], hepatocellular carcinoma cells [31], breast cancer [32] and cervical cancer cells [33, 34]. Recently, we has identified that PG treatment, with an IC50 of 800 μM at 24 h, inhibits the growth of lung cancer cells, particularly A549 epithelial adenocarcinoma cells through apoptosis and/or necrosis [35]. Fibroblasts are the most abundant cell type in the lung interstitium. Pulmonary fibroblasts (PF) play a crucial role in repair and remodeling following injury to the lung [36]. Inadequate or unnecessary accumulation of fibroblasts can result in abnormal tissue function and inflammation [36]. However, little is known about the cytotoxicological effects of PG on normal primary PF cells. Moreover, there are no reports on the relationship between cell death and MAPK signaling in PG-treated normal PF cells. Therefore, elucidating the cytotoxicological effect of PG on apoptosis and MAPK signaling in normal PF cells is important.

The present study aimed to explore the impact of PG exposure within the range of 100–1,600 μM on cell cycle distributions and the death of primary human PF (HPF) cells. Additionally, the study aimed to investigate the influence of various caspase inhibitors and small interfering RNAs (siRNAs) targeting apoptosis-related pathways on PG-induced cell death in HPF cells. Furthermore, the study examined the potential effects of MAPK inhibitors, including MEK (PD98059), JNK (SP600125), and p38 (SB203580) inhibitors, on cell death and the loss of MMP (ΔΨm) in PG-treated HPF cells. The results reveal that PG induces G1 phase arrest and cell death in HPF cells through apoptosis and/or necrosis, with cell death being mitigated by Bax and caspase-3 siRNAs. Notably, MAPK inhibitors do not affect PG-induced cell death or MMP (ΔΨm) loss in HPF cells.

2. Materials and methods

2.1. Cell culture

The primary HPF cells were purchased from PromoCell GmbH (C-12360, Heidelberg, Germany). According to the catalog information from PromoCell GmbH, these cells are derived from human lung tissue, with a

passage number of two post-thawing. The cells were nurtured in RPMI-1640 medium supplemented with 10% fetal bovine serum (FBS; Sigma-Aldrich Co., St. Louis, MO, USA) and 1% penicillin–streptomycin (GIBCO BRL, Grand Island, NY, USA). Cultures were maintained in a humidified incubator with 5% CO2 at 37 °C. Experiments were conducted using HPF cells within the passage range of four to eight.

2.2. Reagents

PG, obtained from Sigma-Aldrich Co. (CAS Number: 121-79-9), is a compound with the molecular formula C10H12O5 and a molecular weight of 212.20. Its purity, determined through HPLC analysis, is guaranteed to be 98% or higher. The inhibitors of pan-caspase (Z-VAD-FMK; benzyloxycarbonyl-Val-Ala-Asp-fluoromethylketone) and caspase-3 (Z-DEVD-FMK; benzyloxycarbonyl-Asp-Glu-Val-Asp-fluoromethylketone), caspase-8 (Z-IETD-FMK; benzyloxycarbonyl-Ile-Glu-Thr-Asp-fluoromethylketone), and caspase-9 (Z-LEHD-FMK; benzyloxycarbonyl-Leu-Glu-His-Asp-fluoromethylketone) were purchased from R&D Systems, Inc. (Minneapolis, MN) and dissolved in dimethyl sulfoxide (DMSO, Sigma-Aldrich Co.) to generate 10 mM stock solutions. MEK (PD98059), JNK (SP600125), and p38 (SB203580) inhibitors were obtained from Calbiochem (San Diego, CA, USA) and dissolved in DMSO at 10 mM. Cells were pretreated with each caspase or MAPK inhibitor for 30 or 60 min prior to treatment with PG. Ethanol (0.2%) and DMSO (0.3%) were used as vehicle controls. All stock solutions were wrapped in foil and kept at 4 °C or −20 °C.

2.3. Cell cycle and sub-G1 cell analysis

Cell cycle and sub-G1 distributions of cells were determined using propidium iodide (PI, Sigma-Aldrich Co.; Ex/Em = 488 nm/617 nm) staining, as previously described [37]. Briefly, 1×10^6 cells in 60-mm culture dishes (BD Falcon) were incubated with the designated concentrations of PG for 24 h. Cells were washed with phosphate buffered saline (PBS; GIBCO BRL) and then incubated with 10 µg/mL PI with RNase (Sigma-Aldrich Co.) at 37 °C for 30 min. The proportions of cells in different phases of the cell cycle or with sub-G1 DNA content were measured and analyzed with a FACStar flow cytometer (BD Sciences, Franklin Lakes, NJ).

2.4. Annexin V/PI staining for cell death detection

Cell death (apoptosis or necrosis) was detected using annexin V-fluorescein isothiocyanate staining (FITC, Life Technologies, Carlsbad, CA; Ex/Em = 488 nm/519 nm), either alone or in combination with PI, as outlined in a previous study described [37]. Briefly, 1×10^6 cells in 60-mm culture dishes (BD Falcon) were preincubated with each caspase inhibitor (15 µM) or MAPK inhibitor (10 µM) for 30 or 60 min prior to treatment with the indicated amounts of PG (100–1,600 µM) for 24 h. Cells were washed twice with cold PBS and then suspended in 200 µL of binding buffer (10 mM HEPES/NaOH pH 7.4, 140 mM NaCl, 2.5 mM $CaCl_2$) at a concentration of 5×10^5 cells/mL at 37 °C for 30 min. Annexin V-FITC (2 µL) and PI (1 µg/ml) were added to the solution, and cells were analyzed using a FACStar flow cytometer (BD Sciences).

2.5. Measurement of MMP (ΔΨm)

The MMP (ΔΨm) was monitored using rhodamine 123 (Sigma-Aldrich Co.; Ex/Em = 485/535 nm), which is a fluorescent, cell-permeable, cationic dye that favorably enters mitochondria with highly negative MMP (ΔΨm). Depolarization of MMP (ΔΨm) results in rhodamine 123 loss from the mitochondria and reduces the intracellular fluorescence intensity of this dye, as previously described [37]. Briefly, 1×10^6 cells in 60-mm culture dishes (BD Falcon) were preincubated with each caspase inhibitor (15 µM) or MAPK inhibitor (10 µM) for 30 or 60 min prior to treatment with the indicated amounts of PG (100–1,600 µM) for 24 h. Cells were washed twice with PBS and incubated with rhodamine 123 (0.1 mg/mL) at a concentration of 5×10^5 cells/mL at 37 °C for 30 min. Rhodamine 123 staining intensities were determined using a FACStar flow cytometer. Rhodamine 123-negative (-) cells indicate MMP (ΔΨm) loss in HPF cells. MMP (ΔΨm) levels in cells without MMP (ΔΨm) loss were expressed as percentages compared with control cells.

2.6. Transfection of cells with apoptosis-related siRNAs

Silencing of apoptosis-related genes, including p53, Bax, Bcl-2, caspase-3, and caspase-8, was performed as previously described [38, 39]. A non-specific control siRNA duplex [5′-CCUACGCCACCAAUUUCGU(dTdT)-3′], p53 siRNA duplex [5′-CACUACAACUACAUGUGUA(dTdT)-3′], Bax siRNA duplex [5′-GCUGGACAUUGGACUUCCU(dTdT)-3′], Bcl-2 siRNA duplex [5′-CAGAAGUCUGGGAAUCGAU(dTdT)-3′], caspase-3 siRNA duplex [5′-AGUAUGCCGAC AAGCUUGA(dTdT)-3′] and caspase-8 siRNA duplex [5′-GCUGCUCUUCCGAAUUAAU(dTdT)-3′] were obtained from the Bioneer Corporation (Daejeon, South Korea). In brief, 2.5×10^5 cells in six-well plates (Nunc, Roskilde,

Denmark) were incubated in RPMI-1640 media supplemented with 10% FBS. The next day, cells (at approximately 30%–40% confluence) were transfected with the control or each siRNA duplex [80 picomoles in Opti-MEM (GIBCO BRL)] using LipofectAMINE 2000, according to the manufacturer's instructions (Invitrogen, Carlsbad, CA). One day later, cells were treated with either PG (800 μM) or a solvent control for an additional 24 or 48 h. Transfected cells were collected and used to measure annexin V-FITC/PI staining.

2.7. Statistical analysis

The results represent the mean of two or three independent experiments (mean ± SD). The data were analyzed using Instat software (GraphPad Prism 5.0, San Diego, CA). A Student's *t*-test or one-way analysis of variance with post hoc analysis using Tukey's multiple comparison test was used to assess statistical significance, which was defined as $p < 0.05$.

3. Results

3.1. Effects of PG on the cell cycle distributions and cell death in HPF cells

The percentages of cells in different stages of the cell cycle were observed after 24 h of incubation with 100–1,600 μM PG. DNA flow cytometric analysis indicated that the doses of PG tested significantly induced G1 phase arrest of the cell cycle in HPF cells, as compared with untreated control cells (Figure 1A and B). The number of cells in S phase of the cell cycle decreased in PG-treated HPF cells (Figure 1A and B).

The assessment of cell death induction through PG treatment was conducted by analyzing sub-G1 cells and annexin V-staining. As shown in Figure 1A and C, 100–800 μM PG treatment did not result in an increase in the number of sub-G1 cells. However, treatment with 1,600 μM PG seemed to elevate the sub-G1 cell population (Figure 1A and C). In addition, 100–200 μM PG did not significantly increase the amount of annexin V-positive HPF cells (Figure 2A and C). However, the amount of annexin V-positive HPF cells increased after incubation with 400–1,600 μM PG (Figure 2A and C). After exposure to 800 μM PG, the proportion of annexin V-positive cells was approximately 20% (Figure 2A and C).

3.2. Effects of PG on MMP (ΔΨm) in HPF cells

Cell death through apoptosis or necrosis is closely associated with the loss of MMP (ΔΨm). In PG-treated HPF cells, this was assessed using rhodamine 123 dye. MMP (ΔΨm) loss in HPF cells was significantly induced by PG at concentrations of 400–1,600 μM after 24 h (Figure 2B and D). After exposure to 800 μM PG, the proportion of HPF cells with MMP (ΔΨm) loss was approximately 30% (Figure 2B and D). Treatment with 100–1,600 μM PG led to a dose-dependent reduction in MMP (ΔΨm) in live HPF cells at 24 h (Figure 2B and E). The MMP (ΔΨm) in HPF cells treated with 100 and 800 μM PG was approximately 60% and 40% as compared with untreated control cells, respectively (Figure 2B and E).

3.3. Effects of caspase inhibitors on cell death and MMP (ΔΨm) loss in PG-treated HPF cells

The effects of caspase inhibitors on cell death and MMP (ΔΨm) loss in PG-treated HPF cells were examined at 24 h. Based on previous experiments related to caspase inhibitors [37, 40], cells were pretreated with inhibitors of pan-caspase (Z-VAD-FMK) and caspase-3 (Z-DEVD-FMK), caspase-8 (Z-IETD-FMK), or caspase-9 (Z-LEHD-FMK) at a concentration of 15 μM for 1 h before exposure to 800 μM PG, a concentration suitable for distinguishing changes in cell death and MMP (ΔΨm) loss in the presence or absence of each caspase inhibitor. None of the caspase inhibitors significantly affected the levels of annexin V-positive PG-treated HPF cells, and the inhibitor of caspase-9 slightly increased the number of annexin V-positive cells (Figure 3A and C). None of the caspase inhibitors tested altered the proportion of cells with MMP (ΔΨm) loss in PG-treated HPF cells (Figure 3B and D).

3.4. Effects of apoptosis-related siRNAs on cell death in PG-treated HPF cells

Next, the impact of apoptosis-related siRNAs against p53, Bax, Bcl-2, caspase-3, and caspase-8 on the levels of cell death in PG-treated HPF cells was evaluated after 24 and 48 h of treatment. The same siRNA sequences targeting p53, Bax, Bcl-2, caspase-3, and caspase-8 were successfully utilized in HPF cells [39, 41]. As depicted in Figure 4, the flow cytometry chart presented serves as a representative figure from the experiments involving annexin V/PI staining for the detection of cell death. Distinguishing between PI-positive (indicating late apoptotic or necrotic cells) and PI-negative (representing early apoptotic cells) within annexin V-positive cells posed a challenge. Therefore, annexin V-positive cells were considered as dead cells, regardless of PI positivity or negativity. As shown in Figure 4A and B, approximately 30% of HPF cells treated with 800 μM PG were annexin

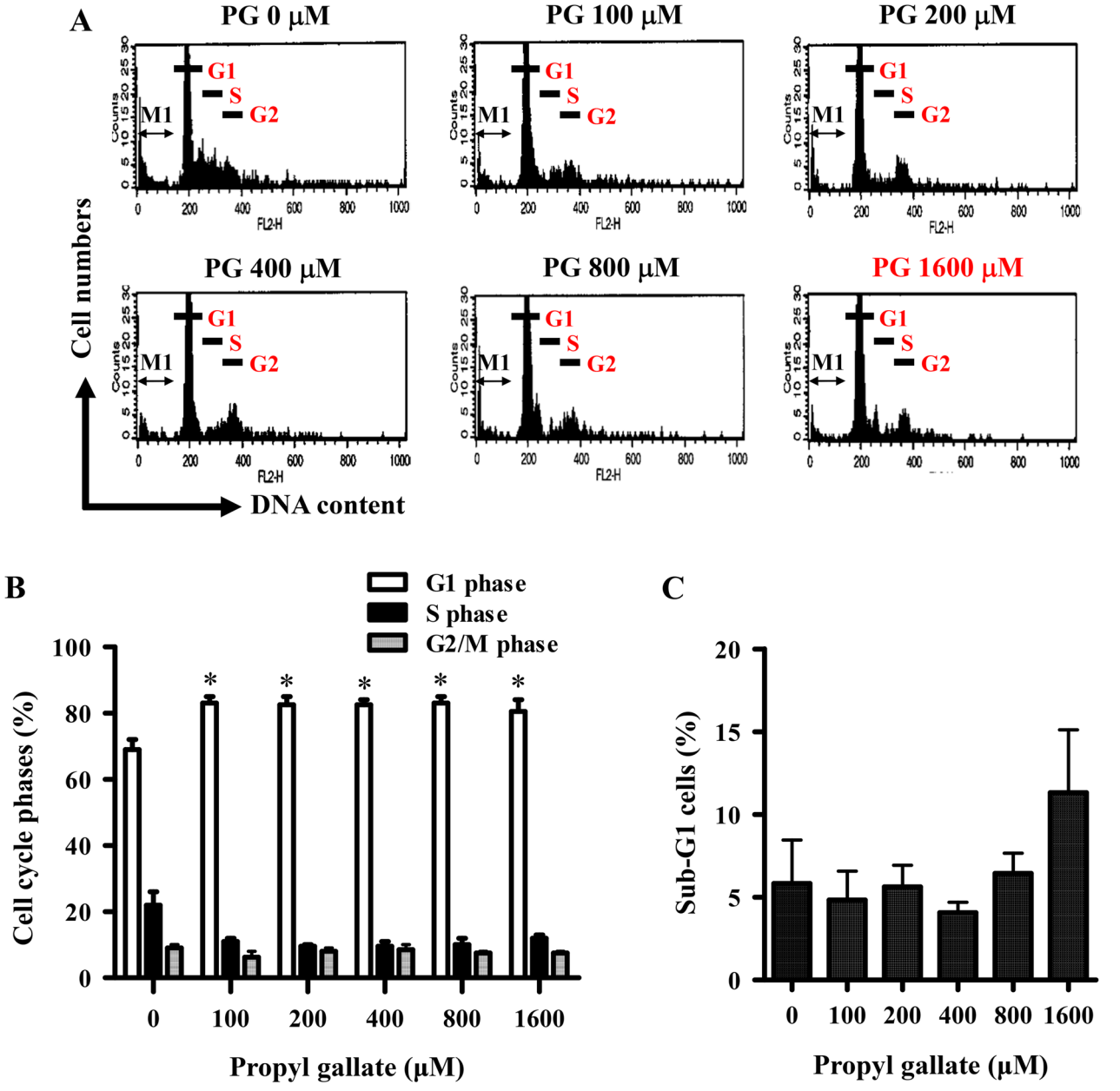

Figure 1. Effects of PG on cell cycle phase distributions in HPF cells. Cells in the exponential growth phase were incubated in the presence of the designated concentrations of PG for 24 h. Cell cycle phase distributions were evaluated by DNA flow cytometry. A: Each histogram shows the cell cycle distributions in PG-treated HPF cells. M1 indicates sub-G1 cells. G1, S, and G2 represent the phases of the cell cycle. B: Graph displaying the proportions of each cell cycle phase derived from A. C: Graph displaying the proportions of sub-G1 cells derived from A. *$p < 0.05$ as compared with untreated control cells.

V-FITC-positive at both 24 and 48 h. The percentage of the annexin V-FITC-positive cells at 24 h was unexpectedly higher, likely attributed to the LipofectAMINE 2000 reagent and variations in cell seeding conditions, which appeared to influence the cell death response to PG. Treatment with Bcl-2, caspase-3, or caspase-8 siRNA seemed to increase the number of annexin V-FITC-positive cells in untreated control HPF cells at both 24 and 48 h, with a more pronounced effect at 24 h (Figure 4A and B). In addition, Bax siRNA slightly increased the number of annexin V-FITC-positive cells in the control cells at 24 h, while this siRNA resulted in a decrease in the annexin V-FITC-positive cell number in the control cells at 48 h (Figure 4A and B). At 24 h, Bax siRNA did not influence the annexin V-FITC-positive cell number in PG-treated HPF cells, but it decreased the number at 48 h (Figure 4A and B). Caspase-3 siRNA somewhat decreased the annexin V-FITC-positive cell number in PG-treated HPF cells at 24 h but did not alter the number at 48 h (Figure 4A and B). At 24 or

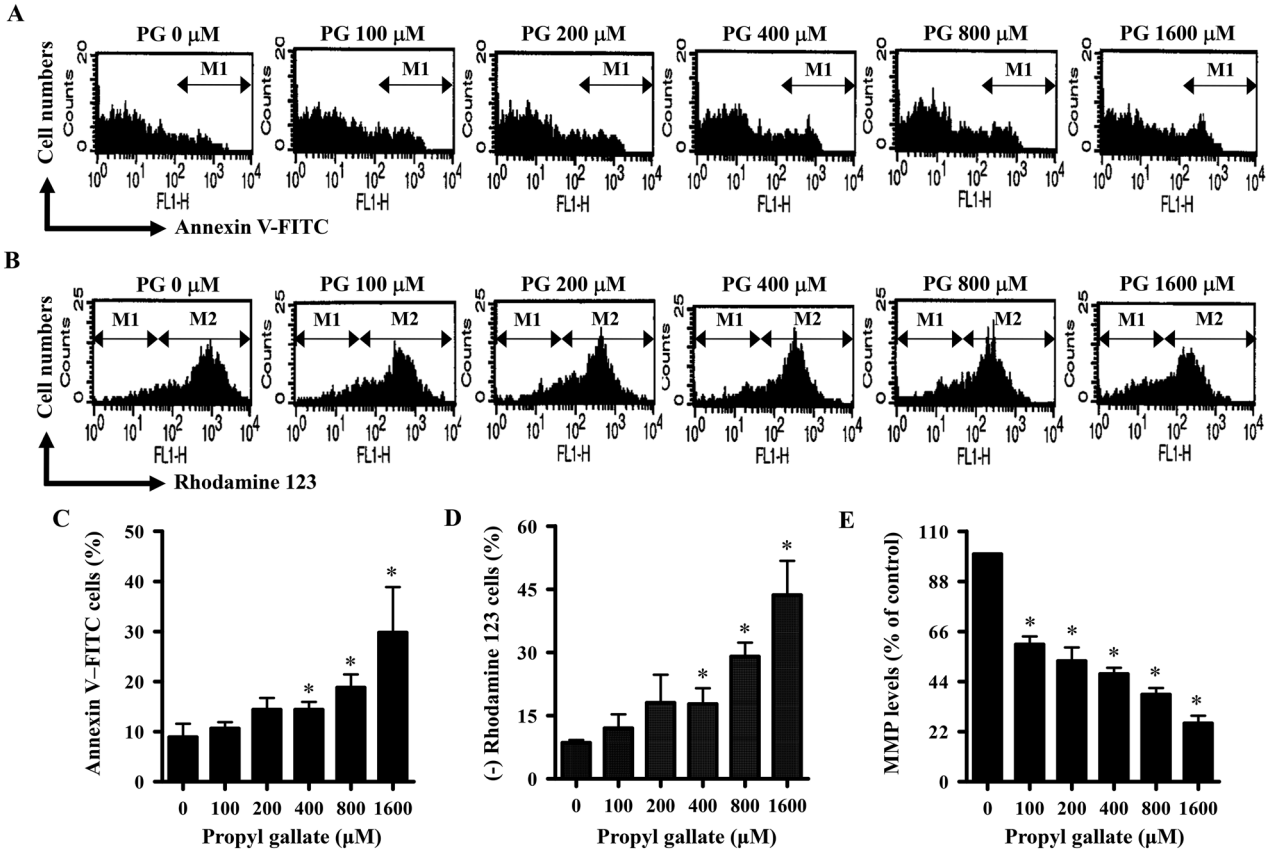

Figure 2. Effects of PG on cell death and MMP (ΔΨm) in HPF cells. Exponentially growing cells were incubated in the presence of the designated concentrations of PG for 24 h. Annexin V-FITC and rhodamine staining were performed in HPF cells and were measured using a FACStar flow cytometer. A and B: Representative histograms for annexin V-FITC (A) and rhodamine staining in HPF cells (B). M1 indicates annexin V-FITC-positive (A) and rhodamine 123-negative [MMP ($\Delta\Psi_m$) loss] HPF cells (B). M2 indicates cells without MMP (ΔΨm) loss. C and D: Graphs of the percentages of M1 regions in A (C) and B (D). E: Graph displaying the proportions of MMP (ΔΨm) levels in HPF cells derived from M2 regions in B. *$p < 0.05$ as compared with untreated control cells.

48 h, p53, Bcl-2, and caspase-8 siRNAs did not affect the number of annexin V-FITC-positive PG-treated HPF cells (Figure 4A and B).

3.5. Effects of MAPK inhibitors on cell death and MMP (ΔΨm) loss in PG-treated HPF cells

The effect of MAPK (MEK, JNK, and p38) inhibitors on cell death and MMP (ΔΨm) loss in PG-treated HPF cells was examined. HPF cells were pretreated with each MAPK inhibitor at a concentration of 10 μM for 30 min, following the protocol from previous experiments related to MAPK inhibitors [42, 43]. Subsequently, the cells were exposed to 800 μM PG for 24 h. As shown in Figure 5A and C, none of the MAPK inhibitors significantly affected the number of annexin V-positive PG-treated HPF cells, but the p38 inhibitor seemed to increase the number of annexin V-positive cells. In addition, none of the MAPK inhibitors significantly altered the proportions of PG-treated HPF cells with MMP (ΔΨm) loss, but the JNK inhibitor slightly augmented MMP (ΔΨm) loss in these cells (Figure 5B and D).

4. Discussion

The dormant toxicity of PG has been inspected to assess various *in vivo* or *in vitro* toxicological properties [44–47]. It has been reported that treatment with PG (100–1,600 μM) inhibits the growth of lung cancer cells through apoptosis and necrosis [35]. Additionally, PG (100–800 μM) inhibits the growth of endothelial cells, especially calf pulmonary arterial endothelial cells, through caspase-independent apoptosis [28]. However, little is known about the cytotoxicological effects of PG on normal lung cells, especially fibroblasts. Lung fibroblasts are crucial for maintaining the integrity of the alveolar structure through the repair of injured areas [36]. In the present study, the cytotoxic effects of PG on cell death and changes in cell cycle distribution in HPF cells were examined. Additionally, alterations in the levels of cell death and MMP (ΔΨm) were assessed

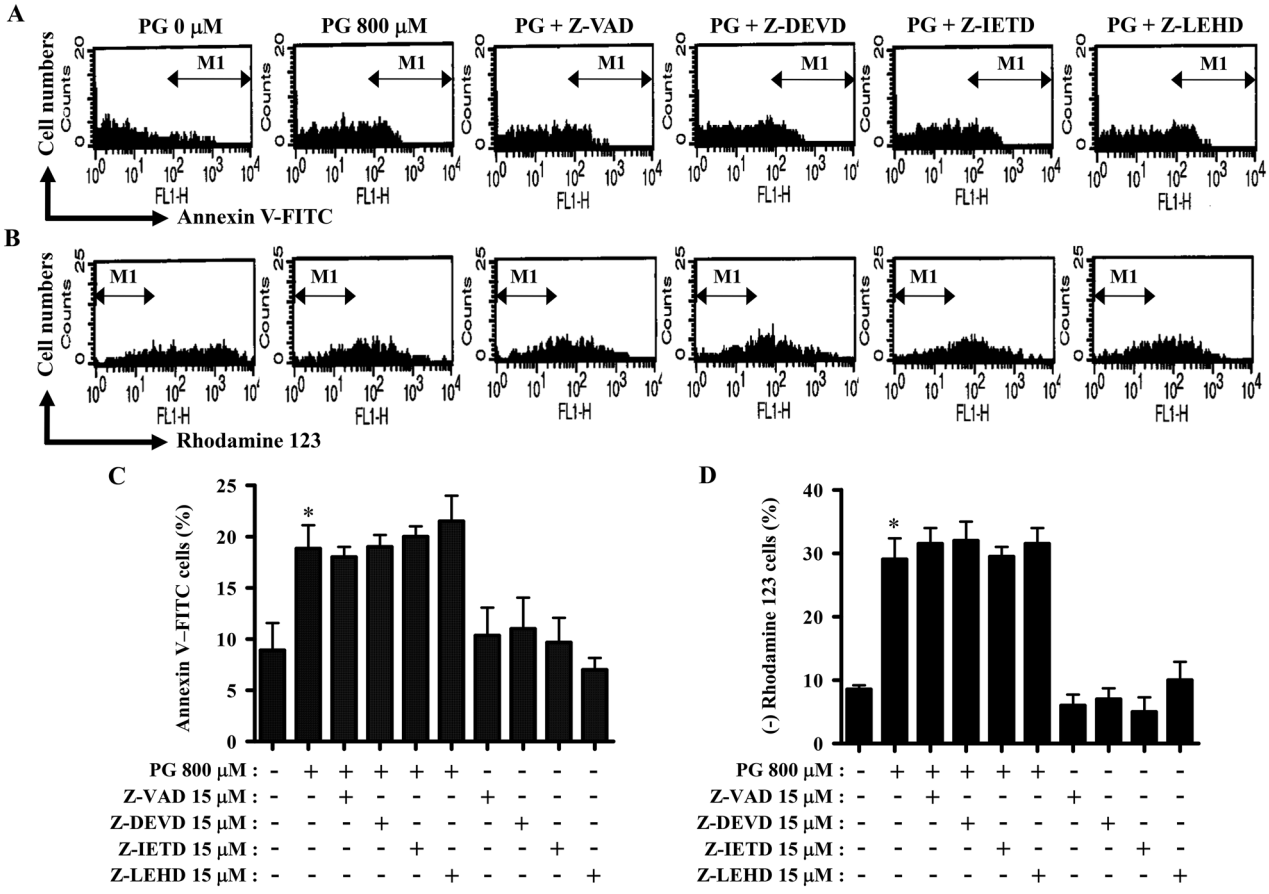

Figure 3. Effects of caspase inhibitors on cell death and MMP (ΔΨm) in PG-treated HPF cells. Exponentially growing cells were pretreated with each caspase inhibitor (15 μM) for 1 h and then treated with 800 μM PG for 24 h. Annexin V-FITC and rhodamine staining were measured in HPF cells using a FACStar flow cytometer. A and B: Representative histograms for annexin V-FITC (A) and rhodamine staining in HPF cells (B). M1 indicates annexin V-FITC-positive (A) and rhodamine 123-negative [MMP (ΔΨm) loss] HPF cells (B). C and D: Graphs show the percentages of M1 regions in A (C) and B (D). *$p < 0.05$ as compared with untreated control cells.

in PG-treated HPF cells with the administration of various caspase inhibitors, apoptosis-related siRNAs, and MAPK inhibitors.

When evaluating the induction of cell death by PG treatment through the analysis of sub-G1 cells and annexin V staining, it was observed that treatment with PG (200–1,600 μM) resulted in a dose-dependent increase in the percentages of annexin V-FITC-positive HPF cells. This implies that cell death induced by PG in HPF cells occurs through apoptosis. Moreover, caspase-3 plays a crucial role in apoptosis. Although the data showing a slight reduction in the level of procaspase-3 in PG-treated HPF cells is not presented, caspase-3 siRNA was observed to somewhat decrease the number of annexin V-FITC-positive cells in PG-treated HPF cells at 24 h. These findings suggest the activation of caspase-3 in these cells. However, treatment with PG (200–800 μM) did not induce the sub-G1 DNA content cells in HPF cells. Furthermore, although PG (1,600 μM) increased the percentage of sub-G1 cells, the effect was insignificant. Therefore, PG appeared to induce HPF cell death *via* apoptosis and/or necrosis, potentially by fixing the cells in a manner similar to ethanol or methanol. DNA flow cytometry indicates that PG induced arrest at the G1 phase of the cell cycle in HPF cells after 24 h of treatment. PG has been shown to induce G1 phase arrest of the cell cycle in HeLa cervical cancer cells after 24 h of treatment [33] and arrest at the G1 phase of the cell cycle in Calu-6 and A549 lung cancer cells after 24 h of treatment [35]. Thus, cell death and the significant G1 phase arrest by PG underlie the growth inhibition of HPF cells.

Cell death *via* apoptosis is related to MMP (ΔΨm) loss [48]. Treatment with PG (400–2,000 μM) has been shown to lead to cell death in various cells by disrupting MMP ($\Delta\Psi_m$) [6, 27, 28, 33]. In addition, the p53 protein controls the expression of Bcl-2 or Bax [14]. A

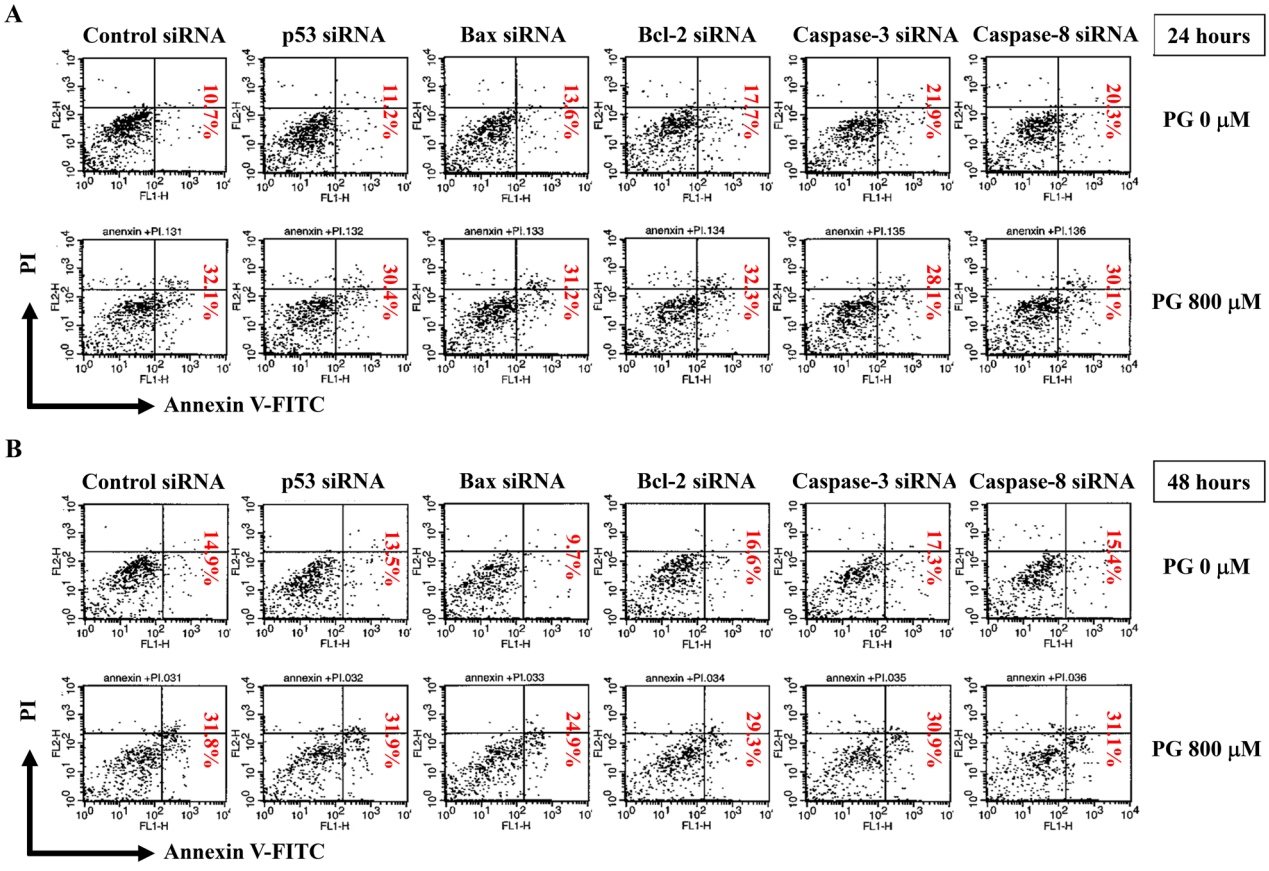

Figure 4. Effects of apoptosis-related siRNAs on cell death in PG-treated HPF cells. HPF cells (at approximately 30%–40% confluence) were transfected with either a nontargeting control siRNA or the indicated apoptosis-related siRNAs. One day later, cells were treated with 800 μM PG for an additional 24 (A) or 48 h (B). A and B: Annexin V-FITC and PI staining in HPF cells were measured using a FACStar flow cytometer. The percentages shown in each figure represent annexin V-FITC-positive cells, regardless of PI-negative and PI-positive cells.

high ratio of Bax/Bcl-2 can lead to MMP ($\Delta\Psi_m$) loss, resulting in the release of cytochrome *c* and apoptosis [48]. Consistent with this, PG led to a dose-dependent reduction in the MMP (ΔΨm) in HPF cells. The degree of MMP (ΔΨm) loss in PG-treated HPF cells was generally higher than that of annexin V-positive cells. For example, after exposure to 800 μM PG, the proportions of annexin V-positive cells and cells with MMP (ΔΨm) loss were approximately 20% and 30%, respectively. These results suggest that PG treatment initially affects the mitochondrial membranes, which precedes the subsequent step for apoptosis. Moreover, when p53, Bax, and Bcl-2 siRNA were pre-administered in PG-treated HPF cells, p53 siRNA led to a decrease in p53 protein levels in HPF cells (data not shown) and did not alter the annexin V-positive cell number in PG-treated or untreated control HPF cells. Thus, the status of p53 might not be related to HPF cell death by PG. Bax siRNA clearly decreased the annexin V-positive cell number in PG-treated and untreated control HPF cells at 48 h. However, Bcl-2 siRNA did not affect the annexin V-positive cell number in PG-treated HPF cells at 24 and 48 h but slightly increased annexin V-positive cell number in HPF control cells. Thus, PG seems to induce MMP (ΔΨm) loss in HPF cells through the regulation of Bax, rather than Bcl-2.

To identify which caspases are required for the induction of cell death, PG-treated HPF cells were incubated with various caspase inhibitors and siRNAs. None of the caspase inhibitors tested in the present study led to decreases in the amounts of annexin V-positive PG-treated HPF cells and also these caspase inhibitors did not alter MMP (ΔΨm) loss in PG-treated HPF cells. Instead, the caspase-9 inhibitor slightly increased the number of annexin V-positive cells, which perhaps resulted from increased necrotic cell death after the interruption of the apoptotic pathway. Caspase-3 siRNA slightly decreased the annexin V-FITC-positive cell number in PG-treated HPF cells at 24 h, whereas caspase-8 siRNA did not affect the cell number in these cells at 24 and 48 h. These results suggest that HPF cell death induced by PG is not highly dependent on the activation of caspases and can be triggered to some extent by the necrotic

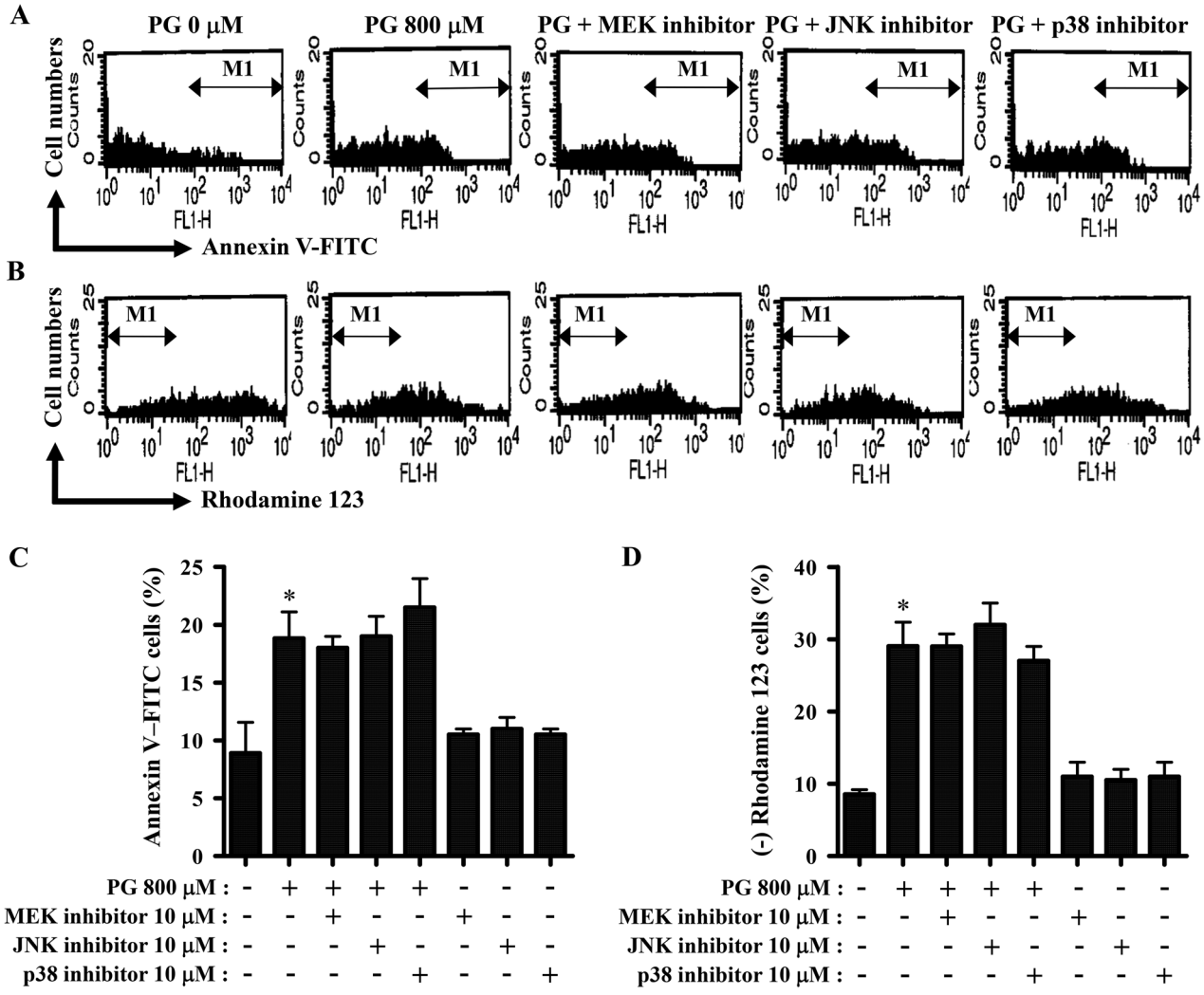

Figure 5. Effects of MAPK inhibitors on cell death and MMP (ΔΨm) in PG-treated HPF cells. Cells undergoing exponential growth were pretreated with each MAPK inhibitor (10 μM) for 30 min and then treated with 800 μM PG for 24 h. Annexin V-FITC and rhodamine staining in HPF cells were measured using a FACStar flow cytometer. A and B: Representative histograms for annexin V-FITC (A) and rhodamine staining in HPF cells (B). M1 indicates annexin V-FITC-positive (A) and rhodamine 123-negative [MMP ($\Delta\Psi_m$) loss] HPF cells (B). C and D: Graphs show the percentages of M1 regions in A (C) and B (D). *$p < 0.05$ as compared with PG-untreated control cells.

pathway. It is noteworthy that caspase-3 and caspase-8 siRNAs increased the annexin V-FITC-positive cell number in untreated control HPF cells, particularly at 24 h, suggesting that the basal activities or levels of caspase-3 and caspase-8 are related to the cell survival of HPF cells. Recent reports suggest that inhibitors of pan-caspase and caspase-3, caspase-8, and caspase-9 significantly prevent PG-induced apoptosis in HeLa cervical cancer cells [34]. In addition, the pan-caspase inhibitor (Z-VAD) also slightly reduced the number of annexin V-positive cells in PG-treated Calu-6 and A549 lung cancer cells [49]. However, in calf pulmonary arterial endothelial cells treated with 400 μM PG, some caspase inhibitors somewhat exacerbated cell death [28]. Therefore, the specific requirements for particular caspases in PG-induced cell death may vary among cell types, particularly between cancer and normal cells.

The ERK signaling pathway is mostly involved in pro-survival, rather than proapoptotic, pathways [20]. The MEK inhibitor, which presumably deactivates ERK, did not increase the number of annexin V-positive cells in PG-treated HPF cells. However, this MEK inhibitor increases the number of annexin V-positive cells in PG-treated HeLa cervical cancer and calf pulmonary arterial endothelial cells [50, 51] and also increases the annexin V-positive cell number in PG-treated Calu-6 lung cancer cells, but not in PG-treated A549 lung cancer cells [52]. These results indicate that PG can induce the death of a certain cell type, especially HPF cells, without influencing ERK signaling. The activation of JNK and p38 has a positive effect on the induction of

apoptosis [22, 23]. However, neither the JNK nor p38 inhibitors tested in the present study decreased the number of annexin V-positive cells in PG-treated HPF cells. Instead, the p38 inhibitor slightly increased the number of annexin V-positive cells. In addition, the JNK and p38 inhibitors appear to increase the number of annexin V-positive cells in PG-treated Calu-6 and A549 lung cancer cells [52]. Therefore, in PG-treated lung cells, including HPF cells, the JNK and p38 signaling pathways are not associated with cell death. Furthermore, none of the MAPK inhibitors significantly altered MMP ($\Delta\Psi_m$) loss in PG-treated HPF cells, suggesting that MAPK signaling pathways are not tightly related to the maintenance of MMP ($\Delta\Psi_m$) in HPF cells.

In conclusion, PG induces G1 phase arrest of the cell cycle and cell death in HPF cells *via* apoptosis and/or necrosis. Although none of the caspase inhibitors attenuated the number of annexin V-positive PG-treated HPF cells, Bax and caspase-3 siRNAs decreased the annexin V-positive cell number in these cells. All of the MAPK inhibitors tested in the present study did not affect PG-induced HPF cell death and MMP ($\Delta\Psi$m) loss. The presented data provides valuable information that aids our understanding of the cytotoxicological and molecular effect of PG on normal lung cells, especially HPF cells. Furthermore, these findings offer insights into the cytotoxic and molecular effects of PG on normal HPF cells, suggesting its potential clinical applicability in both molecular and clinical contexts.

Authors contributions

Woo-Hyun Park is the only author who planned and conducted all experiments and wrote the present paper.

Disclosure statement

The authors declare that they have no known competing financial interests or personal relationships that could have appeared to influence the work reported in this paper.

Ethics declarations

The material in this paper has not been published or is not under active consideration by another journal. The research was conducted in accordance with the declaration of Helsinki.

Funding

The present study was supported by a grant (2019R1I1A2A01041209) of the Basic Science Research Program through the National Research Foundation of Korea (NRF) funded by the Ministry of Education, Republic of Korea.

ORCID

Woo Hyun Park http://orcid.org/0000-0003-4341-5188

Data availability statement

Data collected during the present study are available from the corresponding author upon reasonable request.

References

[1] Final report on the amended safety assessment of propyl gallate. Int J Toxicol. 2007;26(Suppl 3):1–12.
[2] Reddan JR, Giblin FJ, Sevilla M, et al. Propyl gallate is a superoxide dismutase mimic and protects cultured lens epithelial cells from H2O2 insult. Exp Eye Res. 2003;76(1):49–59. doi:10.1016/s0014-4835(02)00256-7.
[3] Chen CH, Liu TZ, Chen CH, et al. The efficacy of protective effects of tannic acid, gallic acid, ellagic acid, and propyl gallate against hydrogen peroxide-induced oxidative stress and DNA damages in IMR-90 cells. Mol Nutr Food Res. 2007;51(8):962–968. doi:10.1002/mnfr.200600230.
[4] Hirose M, Yada H, Hakoi K, et al. Modification of carcinogenesis by alpha-tocopherol, t-butylhydroquinone, propyl gallate and butylated hydroxytoluene in a rat multi-organ carcinogenesis model. Carcinogenesis. 1993;14(11):2359–2364. doi:10.1093/carcin/14.11.2359.
[5] Kobayashi H, Oikawa S, Hirakawa K, et al. Metal-mediated oxidative damage to cellular and isolated DNA by gallic acid, a metabolite of antioxidant propyl gallate. Mutat Res. 2004;558(1-2):111–120. doi:10.1016/j.mrgentox.2003.11.002.
[6] Nakagawa Y, Nakajima K, Tayama S, et al. Metabolism and cytotoxicity of propyl gallate in isolated rat hepatocytes: effects of a thiol reductant and an esterase inhibitor. Mol Pharmacol. 1995;47(5):1021–1027.
[7] Boyd I, Beveridge EG. Relationship between the antibacterial activity towards Escherichia coli NCTC 5933 and the physico-chemical properties of some esters of 3,4,5-trihydroxybenzoic acid (gallic acid. Microbios. 1979;24(97-98):173–184.)
[8] Jacobi H, Eicke B, Witte I. DNA strand break induction and enhanced cytotoxicity of propyl gallate in the presence of copper(II). Free Radic Biol Med. 1998;24(6):972–978. doi:10.1016/s0891-5849(97)00400-0.
[9] Bettger WJ, Ham RG. Effects of non-steroidal anti-inflammatory agents and antioxidants on the clonal growth of human diploid fibroblasts. Prog Lipid Res. 1981;20:265–268. doi:10.1016/0163-7827(81)90052-7.
[10] Martínez-Alonso D, Malumbres M. Mammalian cell cycle cyclins. Semin Cell Dev Biol. 2020;107:28–35. doi:10.1016/j.semcdb.2020.03.009.
[11] Dalton S. Linking the cell cycle to cell fate decisions. Trends Cell Biol. 2015;25(10):592–600. doi:10.1016/j.tcb.2015.07.007.
[12] Chung C. Restoring the switch for cancer cell death: targeting the apoptosis signaling pathway. Am J Health Syst Pharm. 2018;75(13):945–952. doi:10.2146/ajhp170607.
[13] Huska JD, Lamb HM, Hardwick JM. Overview of BCL-2 family proteins and therapeutic potentials. Methods Mol Biol. 2019;1877:1–21.

[14] McCubrey JA, Lertpiriyapong K, Fitzgerald TL, et al. Roles of TP53 in determining therapeutic sensitivity, growth, cellular senescence, invasion and metastasis. Adv Biol Regul. 2017;63:32–48. doi:10.1016/j.jbior.2016.10.001.
[15] Würstle ML, Laussmann MA, Rehm M. The Central role of initiator caspase-9 in apoptosis signal transduction and the regulation of its activation and activity on the apoptosome. Exp Cell Res. 2012;318(11):1213–1220. doi:10.1016/j.yexcr.2012.02.013.
[16] Liu X, Yue P, Zhou Z, et al. Death receptor regulation and celecoxib-induced apoptosis in human lung cancer cells. J Natl Cancer Inst. 2004;96(23):1769–1780. doi:10.1093/jnci/djh322.
[17] Genestra M. Oxyl radicals, redox-sensitive signalling Cascades and antioxidants. Cell Signal. 2007;19(9):1807–1819. doi:10.1016/j.cellsig.2007.04.009.
[18] Kusuhara M, Takahashi E, Peterson TE, et al. p38 kinase is a negative regulator of angiotensin II signal transduction in vascular smooth muscle cells: effects on Na+/H+exchange and ERK1/2. Circ Res. 1998;83(8):824–831. doi:10.1161/01.res.83.8.824.
[19] Blenis J. Signal transduction via the MAP kinases: proceed at your own RSK. Proc Natl Acad Sci U S A. 1993;90(13):5889–5892. doi:10.1073/pnas.90.13.5889.
[20] Henson ES, Gibson SB. Surviving cell death through epidermal growth factor (EGF) signal transduction pathways: implications for cancer therapy. Cell Signal. 2006;18(12):2089–2097. doi:10.1016/j.cellsig.2006.05.015.
[21] Guyton KZ, Liu Y, Gorospe M, et al. Activation of mitogen-activated protein kinase by H2O2. Role in cell survival following oxidant injury. J Biol Chem. 1996;271(8):4138–4142. doi:10.1074/jbc.271.8.4138.
[22] Hsin YH, Chen CF, Huang S, et al. The apoptotic effect of nanosilver is mediated by a ROS- and JNK-dependent mechanism involving the mitochondrial pathway in NIH3T3 cells. Toxicol Lett. 2008;179(3):130–139. doi:10.1016/j.toxlet.2008.04.015.
[23] Mao X, Yu CR, Li WH, et al. Induction of apoptosis by shikonin through a ROS/JNK-mediated process in bcr/abl-positive chronic myelogenous leukemia (CML) cells. Cell Res. 2008;18(8):879–888. doi:10.1038/cr.2008.86.
[24] Latimer HR, Veal EA. Peroxiredoxins in regulation of MAPK signalling pathways; sensors and barriers to signal transduction. Mol Cells. 2016;39(1):40–45. doi:10.14348/molcells.2016.2327.
[25] Hu Z, Li M, Chen Z, et al. Advances in clinical trials of targeted therapy and immunotherapy of lung cancer in 2018. Transl Lung Cancer Res. 2019;8(6):1091–1106. doi:10.21037/tlcr.2019.10.17.
[26] Petty RD, Nicolson MC, Kerr KM, et al. Gene expression profiling in non-small cell lung cancer: from molecular mechanisms to clinical application. Clin Cancer Res. 2004;10(10):3237–3248. doi:10.1158/1078-0432.CCR-03-0503.
[27] Ham J, Lim W, Park S, et al. Synthetic phenolic antioxidant propyl gallate induces male infertility through disruption of calcium homeostasis and mitochondrial function. Environ Pollut. 2019;248:845–856. doi:10.1016/j.envpol.2019.02.087.
[28] Han YH, Moon HJ, You BR, et al. Propyl gallate inhibits the growth of endothelial cells, especially calf pulmonary arterial endothelial cells via caspase-independent apoptosis. Int J Mol Med. 2010;25(6):937–944. doi:10.3892/ijmm_00000425.
[29] Han YH, Moon HJ, You BR, et al. Propyl gallate inhibits the growth of calf pulmonary arterial endothelial cells via glutathione depletion. Toxicol in Vitro. 2010;24(4):1183–1189. doi:10.1016/j.tiv.2010.02.013.
[30] Chen CH, Lin WC, Kuo CN, et al. Role of redox signaling regulation in propyl gallate-induced apoptosis of human leukemia cells. Food Chem Toxicol. 2011;49(2):494–501. doi:10.1016/j.fct.2010.11.031.
[31] Wei PL, Huang CY, Chang YJ. Propyl gallate inhibits hepatocellular carcinoma cell growth through the induction of ROS and the activation of autophagy. PLoS One. 2019;14(1):e0210513. doi:10.1371/journal.pone.0210513.
[32] Tanaka Y, Tsuneoka M. Gallic acid derivatives propyl gallate and epigallocatechin gallate reduce rRNA transcription via induction of KDM2A activation. Biomolecules. 2021;12(1):30. doi:10.3390/biom12010030.
[33] Han YH, Park WH. Propyl gallate inhibits the growth of HeLa cells via regulating intracellular GSH level. Food Chem Toxicol. 2009;47(10):2531–2538. doi:10.1016/j.fct.2009.07.013.
[34] Han YH, Moon HJ, You BR, et al. The anti-apoptotic effects of caspase inhibitors on propyl gallate-treated HeLa cells in relation to reactive oxygen species and glutathione levels. Arch Toxicol. 2009;83(9):825–833. doi:10.1007/s00204-009-0430-2.
[35] Park WH. Propyl gallate reduces the growth of lung cancer cells through caspasedependent apoptosis and G1 phase arrest of the cell cycle. Oncol Rep. 2020;44(6):2783–2791. doi:10.3892/or.2020.7815.
[36] Wilson MS, Wynn TA. Pulmonary fibrosis: pathogenesis, etiology and regulation. Mucosal Immunol. 2009;2(2):103–121. doi:10.1038/mi.2008.85.
[37] Han YH, Kim SZ, Kim SH, et al. Arsenic trioxide inhibits the growth of calu-6 cells via inducing a G2 arrest of the cell cycle and apoptosis accompanied with the depletion of GSH. Cancer Lett. 2008;270(1):40–55. doi:10.1016/j.canlet.2008.04.041.
[38] Park WH. Upregulation of thioredoxin and its reductase attenuates arsenic trioxideinduced growth suppression in human pulmonary artery smooth muscle cells by reducing oxidative stress. Oncol Rep. 2020;43(1):358–367. doi:10.3892/or.2019.7414.
[39] You BR, Park WH. Proteasome inhibition by MG132 induces growth inhibition and death of human pulmonary fibroblast cells in a caspase-independent manner. Oncology Reports. 2011;25(6):1705–1712.
[40] Han YH, Park WH. Proteasome inhibitor MG132 reduces growth of As4.1 juxtaglomerular cells via caspase-independent apoptosis. Arch Toxicol. 2010;84(9):689–698. doi:10.1007/s00204-010-0550-8.
[41] Park WH, Kim SH. Arsenic trioxide induces human pulmonary fibroblast cell death via the regulation of bcl-2 family and caspase-8. Mol Biol Rep. 2012;39(4):4311–4318. doi:10.1007/s11033-011-1218-z.
[42] Han YH, Park WH. Pyrogallol-induced As4.1 juxtaglomerular cell death is attenuated by MAPK inhibitors via preventing GSH depletion. Arch Toxicol. 2010;84(8):631–640. doi:10.1007/s00204-010-0526-8.
[43] You BR, Park WH. The effects of mitogen-activated protein kinase inhibitors or small interfering RNAs on gallic

acid-induced HeLa cell death in relation to reactive oxygen species and glutathione. J Agric Food Chem. 2011;59(2):763–771. doi:10.1021/jf103379d.

[44] Dacre JC. Long-term toxicity study of n-propyl gallate in mice. Food Cosmet Toxicol. 1974;12(1):125–129. doi:10.1016/0015-6264(74)90328-9.

[45] Wu TW, Fung KP, Zeng LH, et al. Propyl gallate as a hepatoprotector in vitro and in vivo. Biochem Pharmacol. 1994;48(2):419–422. doi:10.1016/0006-2952(94)90115-5.

[46] Rosin MP, Stich HF. Enhancing and inhibiting effects of propyl gallate on carcinogen-induced mutagenesis. J Environ Pathol Toxicol. 1980;4(1):159–167.

[47] Abdo KM, Huff JE, Haseman JK, et al. No evidence of carcinogenicity of D-mannitol and propyl gallate in F344 rats or B6C3F1 mice. Food Chem Toxicol. 1986;24(10-11):1091–1097. doi:10.1016/0278-6915(86)90293-0.

[48] Yang J, Liu X, Bhalla K, et al. Prevention of apoptosis by bcl-2: release of cytochrome c from mitochondria blocked. Science. 1997;275(5303):1129–1132. doi:10.1126/science.275.5303.1129.

[49] Park WH. The anti-apoptotic effects of caspase inhibitors in propyl gallate-treated lung cancer cells are related to changes in reactive oxygen species and glutathione levels. Molecules. 2022;27(14):4587. doi:10.3390/molecules27144587.

[50] You BR, Park WH. The enhancement of propyl gallate-induced HeLa cell death by MAPK inhibitors is accompanied by increasing ROS levels. Mol Biol Rep. 2011;38(4):2349–2358. doi:10.1007/s11033-010-0368-8.

[51] Han YH, Kim SZ, Kim SH, et al. Enhancement of propyl gallate-induced calf pulmonary arterial endothelial cell death by MEK and JNK inhibitors. Mol Med Rep. 2009;2(5):825–830. doi:10.3892/mmr_00000179.

[52] Park WH. Enhanced cell death effects of MAP kinase inhibitors in propyl gallate-treated lung cancer cells are related to increased ROS levels and GSH depletion. Toxicol in Vitro. 2021;74:105176. doi:10.1016/j.tiv.2021.105176.